

LETTER • OPEN ACCESS

## Energy potentials and water requirements from perennial grasses on abandoned land in the former Soviet Union

To cite this article: Jan Sandstad Næss *et al* 2022 *Environ. Res. Lett.* **17** 045017

View the [article online](#) for updates and enhancements.

You may also like

- [The global economic long-term potential of modern biomass in a climate-constrained world](#)  
David Klein, Florian Humpenöder, Nico Bauer *et al.*
- [Seasonal energy storage using bioenergy production from abandoned croplands](#)  
J Elliott Campbell, David B Lobell, Robert C Genova *et al.*
- [Responses of \*Alnus nepalensis\* seedling under high phosphorus stress: shifts in photosynthesis and phosphorus contents across different organs](#)  
Zuqing Wu, Mengyang Li, Chengjiao Dao *et al.*



**The Breath Biopsy® Guide**  
Fourth edition

DOWNLOAD THE FREE E-BOOK

BREATH BIOPSY

OWLSTONE MEDICAL

ENVIRONMENTAL RESEARCH  
LETTERS

## LETTER

## OPEN ACCESS

RECEIVED  
15 October 2021REVISED  
7 March 2022ACCEPTED FOR PUBLICATION  
16 March 2022PUBLISHED  
29 March 2022

Original content from  
this work may be used  
under the terms of the  
[Creative Commons  
Attribution 4.0 licence](#).

Any further distribution  
of this work must  
maintain attribution to  
the author(s) and the title  
of the work, journal  
citation and DOI.

Energy potentials and water requirements from perennial grasses  
on abandoned land in the former Soviet UnionJan Sandstad Næss<sup>\*</sup> , Cristina Maria Iordan , Helene Muri and Francesco Cherubini 

Industrial Ecology Programme, Department of Energy and Process Engineering, Norwegian University of Science and Technology, Trondheim, Norway

<sup>\*</sup> Author to whom any correspondence should be addressed.E-mail: [jan.s.nass@ntnu.no](mailto:jan.s.nass@ntnu.no)**Keywords:** bioenergy, abandoned land, land–energy–water nexus, irrigationSupplementary material for this article is available [online](#)

## Abstract

A ramp-up of bioenergy supply is vital in most climate change mitigation scenarios. Using abandoned land to produce perennial grasses is a promising option for near-term bioenergy deployment with minimal trade-offs to food production and the environment. The former Soviet Union (fSU) experienced substantial agricultural abandonment following its dissolution, but bioenergy potentials on these areas and their water requirements are still unclear. We integrate a regional land cover dataset tailored towards cropland abandonment, an agro-ecological crop yield model, and a dataset of sustainable agricultural irrigation expansion potentials to quantify bioenergy potentials and water requirements on abandoned land in the fSU. Rain-fed bioenergy potentials are 3.5 EJ yr<sup>-1</sup> from 25 Mha of abandoned land, with land-sparing measures for nature conservation. Irrigation can be sustainably deployed on 7–18 Mha of abandoned land depending on water reservoir size, thereby increasing bioenergy potentials with rain-fed production elsewhere to 5.2–7.1 EJ yr<sup>-1</sup>. This requires recultivating 29–33 Mha combined with 30–63 billion m<sup>3</sup> yr<sup>-1</sup> of blue water withdrawals. Rain-fed productive abandoned land equals 26%–61% of the projected regional fSU land use for dedicated bioenergy crops in 2050 for 2 °C future scenarios. Sustainable irrigation can bring productive areas up to 30%–80% of the projected fSU land requirements. Unraveling the complex interactions between land availability for bioenergy and water use at local levels is instrumental to ensure a sustainable bioenergy deployment.

## 1. Introduction

Stringent climate change mitigation pathways typically rely on large-scale bioenergy deployment [1]. Median projected land requirements for bioenergy crops in 2100 in 1.5 °C scenarios are in the range of 430–760 million hectares (Mha) [2]. The need to dedicate large areas to bioenergy production for climate change mitigation in such scenarios raises concerns of increasing competition for land resources, deployment feasibility, and potential adverse effects on food security, water scarcity and biodiversity [3–5].

Competition for land with food production and nature conservation limits the land availability for bioenergy. Irrigation of bioenergy crops can ramp up bioenergy supply with reduced land requirements but may pose increased risks of water scarcity [6–8].

Water availability for irrigated bioenergy production is limited by competition for water with irrigated food production, urban water usage, and environmental flow protection [9, 10]. Nexus approaches integrating the interactions between bioenergy potentials, land use, and irrigation water use are key to assess environmental benefits and sustainability trade-offs of bioenergy production [11–13].

Abandoned land has emerged as a crucial option for early bioenergy deployment with reduced trade-offs on the environment and food security relative to targeting areas with primary vegetation or productive croplands [12, 14, 15]. Abandoned land is typically already affected by human activities and located near existing infrastructure as it was previously used for food production. The former Soviet Union (fSU) has experienced major historical land abandonment

over the last 30 years, mainly due to a restructuring of the economy, rural-to-urban migration, decreasing agricultural investments, and access to open markets [16–19]. A recultivation of abandoned land across the fSU may offer an opportunity to ramp-up biomass production [12, 20]. Recent research with a global perspective highlighted the substantial bioenergy potentials for the fSU and relatively high marginal energy gains from irrigation [12, 21]. The fSU also show large expansion opportunities for sustainably deployed agricultural irrigation [22].

Previous land–energy–water nexus assessments of irrigated bioenergy production on abandoned land did not consider if or where the remaining renewable water budget can sustain different levels of new irrigated agricultural activities [12]. It is unclear how sustainable irrigation strategies aiming to protect key environmental water flows can affect bioenergy production potentials. Identifying abandoned land where smaller irrigation infrastructure such as check dams can provide sufficient blue water resources to increase bioenergy productivity may be environmentally preferable to a build-up of larger irrigation infrastructure. There is also a need to investigate green water (i.e. rainfall water in soils available for plant growth) use by bioenergy crops, which is typically underrepresented in the bioenergy scenario literature [23] despite its importance in sustainable water resource management [24, 25].

Studies of bioenergy potentials on abandoned land have so far mainly taken a global scale perspective [12, 21, 26, 27]. They rely on global land cover datasets that typically lack spatially differentiated validation of cropland classes and land use transitions. Regional land cover datasets that are extensively validated and have higher accuracy than global products represents opportunities for refined bioenergy estimates. So far, area-limited studies applying regional land cover datasets are few and have been limited to the United States [28–30]. A regional land cover dataset tailored towards abandoned land has been made available for the fSU [16]. The dataset is validated both at the regional and country level against 5972 datapoints and achieves abandoned land user and producer accuracies of 31% and 62%, respectively. It is therefore an attractive dataset for refined regional assessments.

In this work, we perform a land–energy–water nexus analysis of bioenergy potentials from abandoned land by integrating specific datasets for each of the nexus elements: a recently developed and extensively validated land dataset [16] (land), an agro-ecological crop yield model (global agro-ecological zones (GAEZ) v3.0) [31] (energy), and newly developed spatial datasets of sustainable agricultural irrigation expansion [22] (water). Bioenergy potentials are quantified for two types of perennial grasses, reed canary grass and switchgrass, at rainfed and irrigated conditions and two management

intensities (medium and high management intensities). In addition to fully rainfed and irrigated conditions, we consider three different sustainable irrigation management strategies and quantify their effects on bioenergy potentials and water use. Using country specific confusion matrices describing land cover dataset accuracy for correction [16], we quantify total potentials, and associated land and water use from abandoned land for each country in the fSU.

## 2. Methods

### 2.1. Land availability

We used the land cover map from Lesiv *et al* [16, 32] of arable and abandoned land across the fSU, here referred to as the hybrid map. The abandoned land class (59 Mha) from the hybrid map serves as a basis for land availability. Abandoned land is defined as land previously cultivated before 2010 that is unutilized for more than 5 years. The hybrid map was produced by combining multiple input data sets, including specialized land abandonment data from remote sensing [33–36], series of annual land cover maps [37, 38], and static land cover maps and cropland maps [39, 40]. A Bayesian network was applied to fuse them into one product at 10 arcseconds resolution [16].

Parts of the abandoned land (10%) is located within biodiversity hotspots [41] and protected areas [42] where habitat restoration can be especially beneficial for biodiversity [43, 44] (supplementary text 1 and supplementary figure 1 available online at [stacks.iop.org/ERL/17/045017/mmedia](https://stacks.iop.org/ERL/17/045017/mmedia)). We excluded abandoned land within these areas from the main analysis using masks of biodiversity hotspots [45] and protected areas [31, 42].

For comparisons, we used country masks [46] to filter out future projections of fSU bioenergy land use in 2 °C scenarios from a gridded land cover dataset at 0.05° resolution [47] produced by the global change assessment model [48, 49] and the land use downscaling model DEMETER [50, 51]. These projections cover a comprehensive set of shared socio-economic pathways [52] (SSPs) and representative concentration pathways [53] (RCPs). We considered the harmonized future land use projections for all SSPs with RCP2.6 [54] in 2050 where the temperature target [55] is achieved (all but SSP3).

### 2.2. Water availability

Bioenergy potentials and water requirements are estimated according to different water supply regimes: rainfed conditions, unconstrained irrigation, and three different strategies for sustainable irrigation. The sustainable irrigation strategies are based on a state-of-the-art dataset of candidate areas for sustainable agricultural irrigation expansion from Rosa *et al* [22] that is available at 5 arcmin resolution [56]. We integrated the irrigation expansion dataset

with the hybrid map to identify abandoned land within candidate areas for sustainable agricultural irrigation. Based on the irrigation budgets from the irrigation expansion dataset, we calculated gridded fractions of abandoned land that can be irrigated.

The irrigation expansion dataset identifies irrigation practices as sustainable if their water use does not exceed local renewable water availability of surface and ground water and does not deplete environmental flows or freshwater stocks. It is based on a hydrological analysis done at a grid cell level using historical observational data (1996–2005) of precipitation, water runoff and evaporation [22]. A minimum monthly threshold of 60% of water runoff was allocated to environmental flows, thereby limiting trade-offs on freshwater ecosystems [57, 58]. Cells are classified as candidate areas for irrigation expansion if the remaining renewable water resources can meet total irrigation water requirements from the agricultural sector. It provides spatial recommendations of three irrigation strategies based on a priority list. First, a soft-path scenario with small monthly water storages meeting the necessary irrigation water requirements to avoid all crop water deficits. This is a decentralized approach with small and modular infrastructure that allows productivity benefits whilst minimizing adverse environmental impacts of large irrigation infrastructure. Second, a soft-path deficit irrigation deployment with small monthly storages where only 80% of the irrigation water requirements needed to avoid crop water deficits can be met. Third, hard-path irrigation with large annual storages transferring water both between months and from wet to dry seasons, thereby meeting all irrigation water requirements. Hard-path irrigation requires larger investments to construct large-scale water reservoirs and substantial additional infrastructure, and reservoir storage capacity needs to be larger than dry-season water withdrawals. Grids where none of the irrigation strategies can meet irrigation water requirements are classified as primarily rain-fed.

### 2.3. Bioenergy crop productivity

We consider two perennial grasses switchgrass and reed canary grass (supplementary text 2). Bioenergy crop yields (dry mass) and crop evapotranspiration (water evaporated and transpired from soil and plants to the atmosphere) on abandoned land were quantified at 5 arcmin resolution using data from the parameterized crop model GAEZ v3.0 [31] (supplementary text 3). We consider two different agricultural management intensities with both rain-fed and irrigated water supply. Medium agricultural management intensity refers to cultivation with a partly mechanized system and some fertilizer and pesticide use, and is closer to the dominant practice across the fSU today [12]. High agricultural management intensity represents a modern system with closed yield gaps, full mechanization, improved varieties, and

optimal use of fertilizer and pesticides. For irrigated conditions, we quantified irrigation water requirements needed to avoid water deficits during the crop growth cycle with GAEZ data. Sustainable irrigation strategies (soft-path, soft-path with deficit, and hard-path) considers a mix of rain-fed and irrigated yields, which we allocated spatially based on the irrigation expansion dataset. For soft-path deficit irrigation, we assumed a linear increase in yields with partially added irrigation from fully rain-fed to irrigated conditions [59]. This means that the 80% deficit irrigation provides an 80% increase from rain-fed to fully irrigated yields. We used GAEZ data considering climatic conditions centered around the 2020s (2010–2040) from the Hadley Centre coupled model v3 [60] in the main analysis to remain comparable with previous studies [12, 21]. Additionally, we repeated the analysis considering a measurement based climate input from the Climate Research Unit [61, 62] (1960–1990) to assess how the driving climate data considered by GAEZ affects results. Dry mass crop yields are converted to bioenergy yields using lower heating values of  $17.82 \text{ MJ kg}^{-1}$  for switchgrass and  $18.06 \text{ MJ kg}^{-1}$  for reed canary grass [63].

We compared predicted switchgrass yields from GAEZ with those from a machine learning dataset [64] and from the global hydrological model H08 (v.bio1) [65] (supplementary figure 2 and supplementary text 4). Pixel-based estimates of both reed canary grass and switchgrass yields were additionally compared with observational data found in literature, both at a site-specific and an aggregated country level (supplementary figure 3 and supplementary text 5). Gathered observational data for reed canary grass and switchgrass is shown in supplementary tables 1 and 2, respectively (partly taken from [66]). We also processed yield data of willow, poplar, and eucalypt from the machine learning dataset [64] to assess the potentials of woody bioenergy crops (supplementary figure 4 and supplementary text 6), as they could be an alternative to perennial grasses.

### 2.4. Land–energy–water nexus

Irrigation expansion datasets are integrated with quantified bioenergy yields and land availability maps to assess the effects of different irrigation management strategies on the land–energy–water nexus. We optimized the bioenergy crop distribution for maximum primary energy production per grid cell. In total, we considered 180 different variants of land and water-dependent bioenergy potentials (supplementary table 3). Results in the main text are mainly shown for medium agricultural management intensity, and with land use constraints limited to abandoned land outside protected areas and biodiversity hotspots. Other results are available in the supplementary information.

We quantified mean bioenergy yields and evapotranspiration rates at the country level using country



masks [46]. Based on country-specific confusion matrices from the hybrid map [16, 67], we produced adjusted estimates of total bioenergy potentials, productive areas, and water use across the fSU that consider abandoned land dataset accuracy. We partition between green and blue water use. Green water is water stored locally in the soil recharged by precipitation and available for plant growth, while blue water is water withdrawn for irrigation from lakes, rivers, groundwater or artificially created infrastructure such as reservoirs [24, 68].

The land–energy–water nexus is unraveled by assessing key indicators related to bioenergy yields and land and water use. We map water use efficiency ( $\text{GJ mm}^{-1} \text{ ha}^{-1}$ ) given as the relationship between bioenergy potentials, crop water evapotranspiration (green and blue water), and land requirements, thereby incorporating all the dimensions of the land–energy–water nexus. Similarly, we assess marginal energy gains of irrigation ( $\text{GJ mm}^{-1} \text{ ha}^{-1}$ ), as the relationship between total energy gains of irrigation, irrigated land use, and irrigated blue water use. This indicator includes energy gains from changes in the optimal crop calendar allowed by irrigated water supply and is not directly comparable to water use efficiency. Finally, we show green and blue water footprints ( $\text{m}^3 \text{ GJ}^{-1}$ ), assessing trade-offs between water depletion and increased bioenergy production.

### 3. Results

#### 3.1. Bioenergy potentials, productive land, and water use

Depending on water supply system, the total bioenergy potential from abandoned land range between 3.5 and 16 exajoules ( $\text{EJ yr}^{-1}$ ), assuming optimal crop mix, medium agricultural management intensity, and sparing of protected areas and biodiversity hotspots for nature conservation (figure 1(a)). The associated productive land requirements are 25–53 Mha (figure 1(b)). Green and blue water requirements are 98–192 billion  $\text{m}^3$  and 0–223 billion  $\text{m}^3$ , respectively (figure 1(c)).

The rain-fed bioenergy potential is 3.5  $\text{EJ yr}^{-1}$ . The corresponding green water use is 108 billion  $\text{m}^3 \text{ yr}^{-1}$ , with 19 and 6.3 Mha of land allocated to reed canary grass and switchgrass, respectively. In general, high bioenergy potentials heavily rely on irrigation deployment, which boosts yields and increases productive area extent through increased water use. We find that 18 Mha of the 53 Mha of abandoned land outside biodiversity hotspots and protected areas can be irrigated without breaching grid-box specific water budgets, based on local renewable freshwater availability and environmental flow protection (supplementary figure 5). Implementing sustainable irrigation strategies can double bioenergy potentials relative to rain-fed conditions (figure 1(a)). Introducing soft-path irrigation with

small monthly water storages on 7.8 Mha by applying 30 billion  $\text{m}^3 \text{ yr}^{-1}$  of blue water withdrawals allows adding another 4.4 Mha (or +8%) into production, thereby increasing the bioenergy potential by 1.7  $\text{EJ yr}^{-1}$  (or +49%). Additional soft-path irrigation with water deficits on 2.5 Mha of land increases potentials with another 0.6  $\text{EJ yr}^{-1}$  and blue water use with another 10 billion  $\text{m}^3 \text{ yr}^{-1}$ . Adding hard path irrigation management with large annual water storage deployed on 7.9 Mha further ramps-up bioenergy potentials with 1.3  $\text{EJ yr}^{-1}$  and blue water requirements with 22 billion  $\text{m}^3 \text{ yr}^{-1}$ , respectively. With complete irrigation, a maximum potential of 16  $\text{EJ yr}^{-1}$  is achievable with 223 billion  $\text{m}^3 \text{ yr}^{-1}$  of blue water withdrawals. However, this involves using 160 billion  $\text{m}^3$  of blue water for irrigation where it is classified as unsustainable.

Compared to the land area in the fSU set aside for bioenergy in 2050 across different SSPs for 2 °C scenarios, our estimates of rain-fed productive abandoned land are equal to 26%–61% (figure 1(d)). The inclusion of different sustainable irrigation strategies can bring productive areas up to 30%–80% of it. The highest projected fSU land demand for bioenergy crops is found in SSP5-2.6 with 97 Mha, and productive rain-fed abandoned land equals 26% of it. Different irrigation management strategies increase productive land area to 30%–34% of SSP5-2.6 land requirements, respectively.

With improved agricultural management to close yield gaps (high agricultural management intensity), bioenergy potentials are 3.9–21  $\text{EJ yr}^{-1}$ , or 12%–31% higher than those at medium management intensity across the different water supply systems (supplementary figure 6). The three considered sustainable irrigation strategies achieve potentials between 6.1 and 8.6  $\text{EJ yr}^{-1}$ , with 32–67 billion  $\text{m}^3 \text{ yr}^{-1}$  of blue water withdrawals and 6.6–16.3 Mha of irrigated areas. Whilst total blue water withdrawals for irrigation increase (+7% for all) to meet rising rain-fed crop water deficits per hectare, the total irrigated area extent decreases (−6% to −7%) across irrigation strategies. This is due to blue water budget constraints that limits further water withdrawals to remain sustainable in some locations (supplementary figure 7).

#### 3.2. Bioenergy productivity across water management strategies

With rain-fed water supply at medium agricultural management intensity, reed canary grass is the dominant crop (figure 2). Reed canary grass and switchgrass yields at rain-fed conditions range between 50–200  $\text{GJ ha}^{-1} \text{ yr}^{-1}$  and 150–250  $\text{GJ ha}^{-1} \text{ yr}^{-1}$ , respectively. Crop water deficits are a major constraint to bioenergy productivity across the fSU. With irrigation, nearly all abandoned lands are productive, and switchgrass becomes the highest yielding crop in most locations. Irrigated bioenergy yields mainly range between 150–200  $\text{GJ ha}^{-1} \text{ yr}^{-1}$

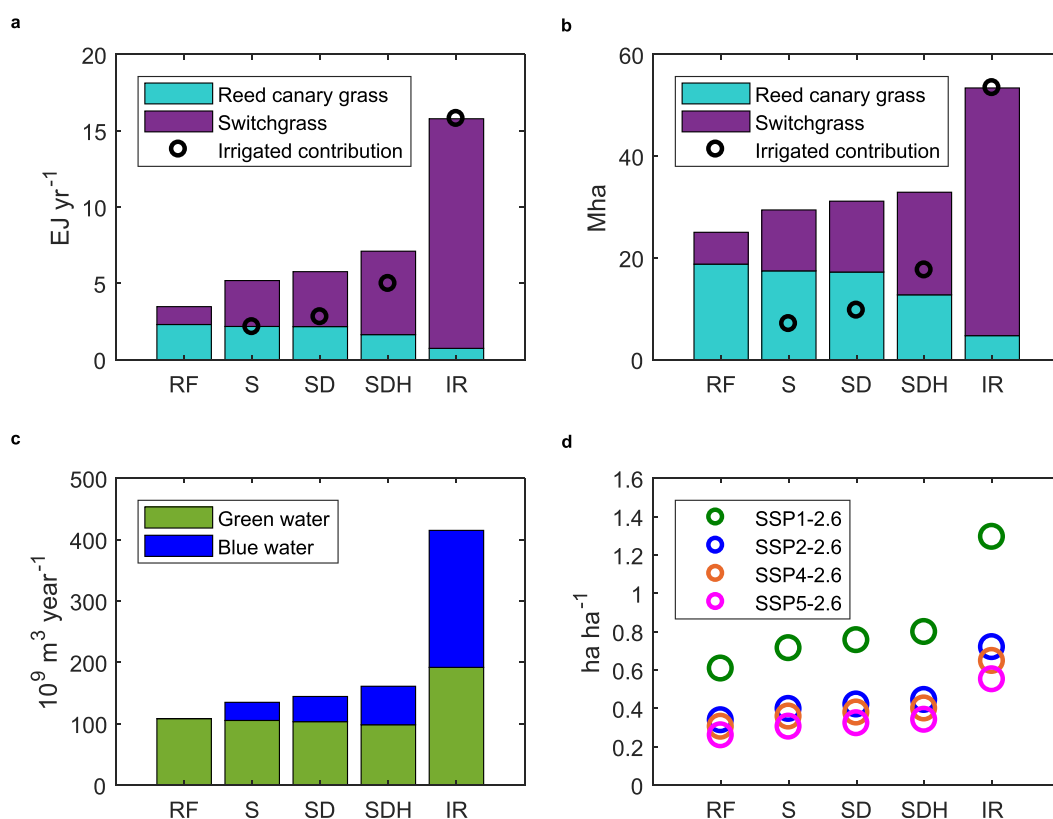


**Figure 1.** Bioenergy potentials and their land and water use requirements across water supply systems. (a) Bioenergy potentials ( $\text{EJ yr}^{-1}$ ). (b) Productive abandoned land (Mha). (c) Crop water use ( $10^9 \text{ m}^3 \text{ yr}^{-1}$ ) originating from green and blue water sources (local precipitation and irrigated water withdrawals, respectively). (d) Total productive abandoned land found here divided by projected SSPx-2.6 fSU bioenergy land use in 2050 ( $\text{ha/ha}$ ). All shown values are adjusted for country-specific land cover dataset confusion matrices. Medium agricultural management intensity is considered. Water supply systems are rain-fed (RF), soft-path irrigation with monthly water storage (S), soft-path irrigation with crop water deficit (D), hard-path irrigation with annual water storage (H), and complete irrigation (IR). Water supply systems applying combinations of S, D, and H considers rain-fed supply on the remaining non-irrigated land. Land use considered refer to abandoned land outside biodiversity hotspots and protected areas. Irrigated part of productive lands and bioenergy potentials are shown in (a) and (b) with an empty black circle.

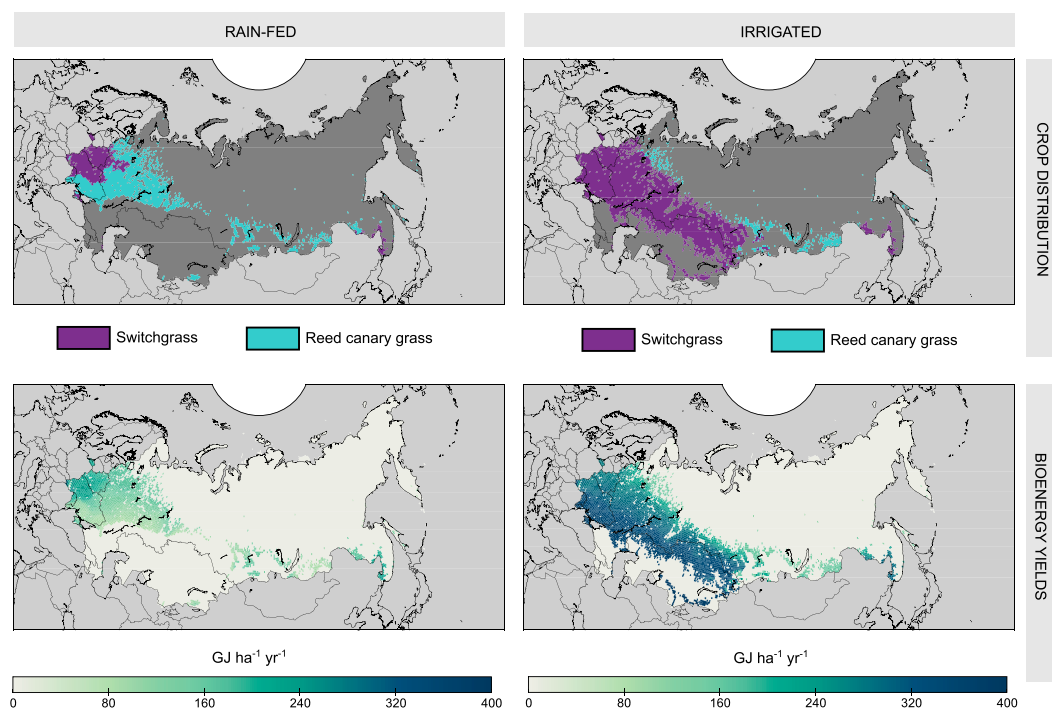
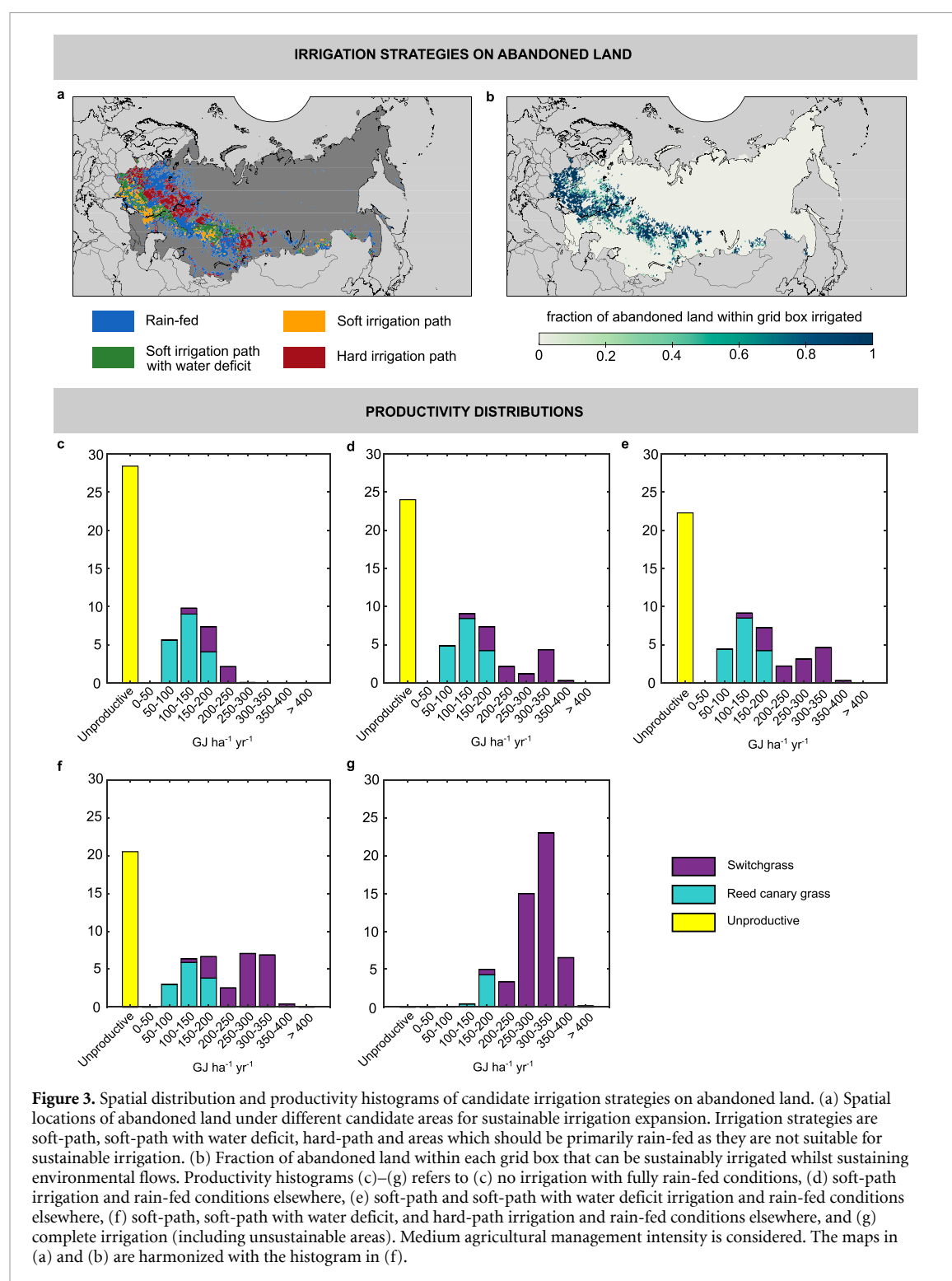


**Figure 2.** Irrigation effects on spatially optimal crop allocation and bioenergy yields at medium agricultural management intensity. Results are shown for rain-fed and irrigated water supply in left and right columns, respectively.



and 200–400  $\text{GJ ha}^{-1} \text{yr}^{-1}$  for reed canary grass and switchgrass, respectively.

In addition to the full irrigation, bioenergy potentials are also explored according to the deployment of three intermediate sustainable irrigation strategies (following [22]) (figure 3 and supplementary figure 8). Considering soft-path and soft-path deficit irrigation approaches with small monthly water storages, we find suitable areas mainly north of the Black Sea, Northern Kazakhstan, in addition to some smaller

clusters in Eastern Russia (figure 3(a)). A hard irrigation path with large annual storages can be considered around the middle and upper Volga region and in parts of Belarus.

At rain-fed conditions the mean bioenergy yield is 139  $\text{GJ ha}^{-1} \text{yr}^{-1}$  with 28 Mha left unproductive (figure 3(c)). Reed canary grass and switchgrass have mean bioenergy yields of 122 and 187  $\text{GJ ha}^{-1} \text{yr}^{-1}$ , respectively. Soft-path irrigation (figure 3(d)) increases the mean bioenergy yield to

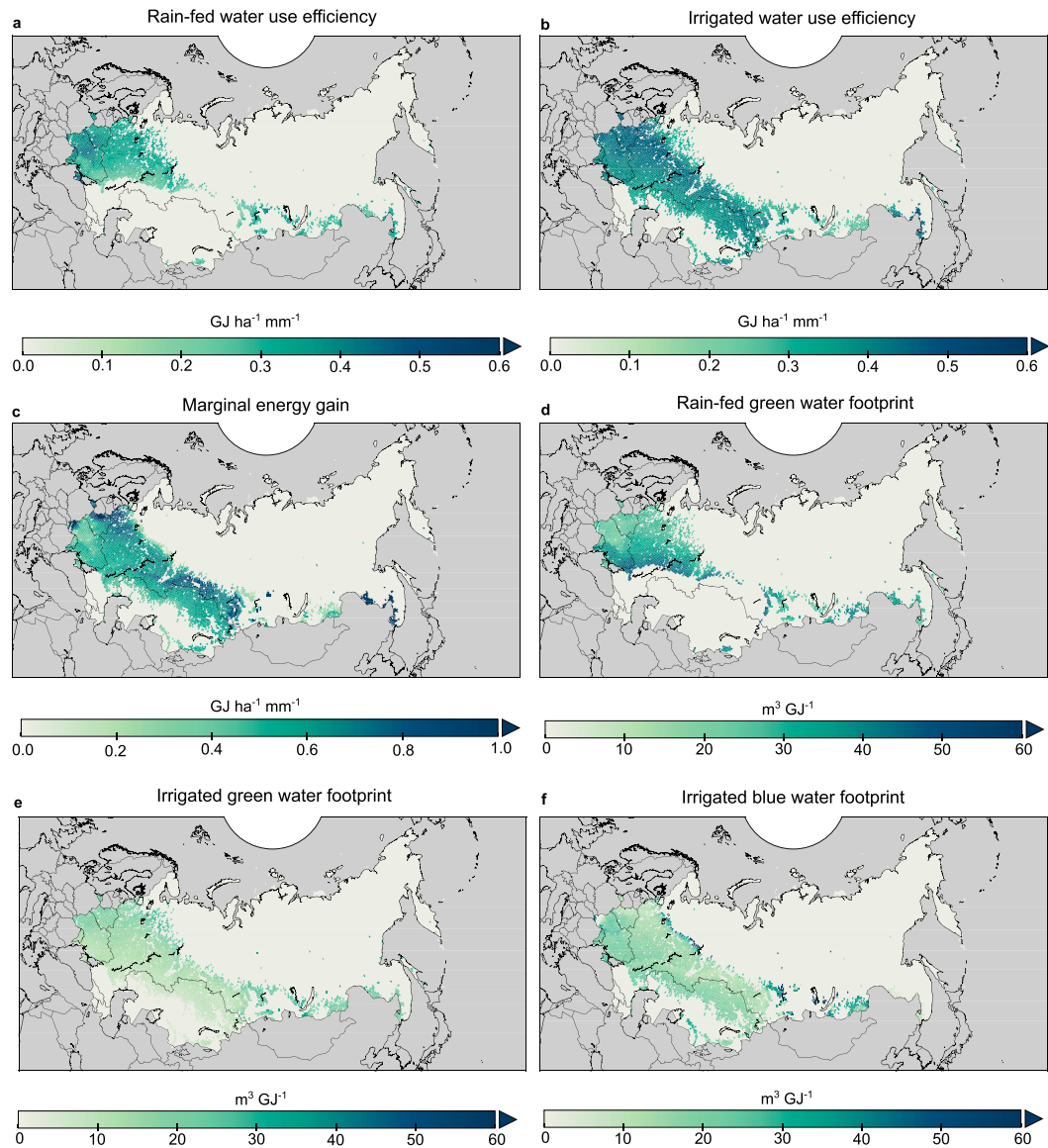


**Figure 4.** Land–energy–water interactions of deploying bioenergy with optimal crop allocation and medium management intensity. (a) Water use efficiency at rain-fed conditions. (b) Water use efficiency at irrigated conditions. (c) Marginal energy gain of irrigation deployment. (d) Green water footprint at rain-fed conditions. (e) Green water footprint at irrigated conditions. (f) Blue water footprint at irrigated conditions. The blue water footprint is given here as the blue water use per unit energy gained at irrigated conditions relative to at rain-fed conditions.

176 GJ ha<sup>-1</sup> yr<sup>-1</sup>, while additionally considering soft-path deficit irrigation (figure 3(e)) and hard-path irrigation (figure 3(f)) increases means to 185 and 216 GJ ha<sup>-1</sup> yr<sup>-1</sup>, respectively. Deploying all three paths reduces unproductive areas to 21 Mha (–25%). Mean switchgrass yields increase more than reed canary grass yields relative to rain-fed conditions (to 271 and 128 GJ ha<sup>-1</sup> yr<sup>-1</sup> (or +45% and +5%), respectively). With complete irrigation (figure 3(g)) mean bioenergy yields are 296 GJ ha<sup>-1</sup> yr<sup>-1</sup>, but it implies irrigating areas where blue water withdrawals are unsustainable or where blue water might not be locally available.

Large productive areas with rain-fed water supply are found in Russia (21 Mha) and Ukraine (2.9 Mha), with bioenergy potentials of 2.8 and 0.5 EJ yr<sup>-1</sup>, and mean bioenergy yields of 133 and

164 GJ ha<sup>-1</sup> yr<sup>-1</sup> (supplementary table 4). Kazakhstan has limited productive areas at rain-fed conditions (0.3 Mha), and different sustainable irrigation management strategies can substantially favor bioenergy productivity (up to 3.6 Mha of land can become productive with a potential of 1.0 EJ yr<sup>-1</sup>).

### 3.3. Spatial land–energy–water interactions

Water use efficiencies range between 0.2 and 0.5 GJ ha<sup>-1</sup> mm<sup>-1</sup> at rain-fed conditions and medium management intensity (figure 4(a)). Water use efficiencies are typically higher with switchgrass than reed canary grass. With irrigation, the combined use of green and blue water increases water use efficiencies to above 0.3 GJ ha<sup>-1</sup> mm<sup>-1</sup> everywhere with a fsu mean of 0.38 GJ ha<sup>-1</sup> mm<sup>-1</sup> (figure 4(b)). This

is due to more land being allocated to switchgrass and to changing crop calendars.

Marginal energy gains of irrigation mainly range between 0.3 and 1 GJ ha<sup>-1</sup> mm<sup>-1</sup> (figure 4(c)). Marginal energy gains are especially high in the very western part of the fSU, in Eastern Russia and in Russia–Kazakhstan border areas. Lower marginal energy gains below 0.5 GJ ha<sup>-1</sup> mm<sup>-1</sup> are found in Siberia, and southern parts of Kazakhstan.

Blue water withdrawals for irrigation also affect green water use as it can allow for a crop change or make new areas cultivable. At rain-fed conditions, green water footprints are primarily between 20 and 50 m<sup>3</sup> GJ<sup>-1</sup>, with a mean of 31 m<sup>3</sup> GJ<sup>-1</sup> (figure 4(d)). Spatially, the green water footprint is higher in areas allocated to reed canary grass than to switchgrass. We find decreasing green water footprint with irrigation across the fSU to 0–30 m<sup>3</sup> GJ<sup>-1</sup> with a mean of 12 m<sup>3</sup> GJ<sup>-1</sup> (figure 4(e)). Green water footprints are above 20 m<sup>3</sup> GJ<sup>-1</sup> only at high latitudes and in the Eastern parts of Russia. In areas with relatively low green water footprint the crop water use is dominated by irrigated blue water, such as in large parts of Kazakhstan. Blue water footprints are between 10 and 40 m<sup>3</sup> GJ<sup>-1</sup>, with a fSU mean of 18 m<sup>3</sup> GJ<sup>-1</sup> (figure 4(f)). The highest blue water footprints are found in Siberia. Of the three sustainable irrigation strategies, soft path deficit irrigation has the highest blue water footprint with 20 m<sup>3</sup> GJ<sup>-1</sup>, while soft and hard-path irrigation have means of 17 and 16 m<sup>3</sup> GJ<sup>-1</sup>, respectively (caused by the differences in spatial distribution of the irrigation strategies).

Irrigation can be an especially attractive option where smaller water reservoirs can provide enough blue water for (deficit) irrigation and where bioenergy yield gains per unit of supplied water is relatively high. Clusters with both marginal energy gains of irrigation in the top quartile and soft-path or soft-path with deficit irrigation opportunities are found in Russia–Kazakhstan border areas, in the far west of Ukraine, and in Eastern Russia.

#### 4. Discussion and conclusions

Our study finds higher bioenergy potentials (3.5–23 EJ yr<sup>-1</sup> across 180 scenarios) from abandoned lands in the fSU than in previous studies (0.7–3.8 EJ yr<sup>-1</sup>) [12, 21] that used a global land cover product to identify abandoned cropland (supplementary table 5). To isolate the role of the land cover dataset, we used the same yield model and considered the same climatic conditions and agricultural management intensities as in those previous studies. The increase in potential found here is attributable to the use of a validated regional land cover dataset tailored for land abandonment monitoring, which is a clear advance relative to global land cover datasets [16, 67].

There are still a variety of uncertainties and limitations that can affect our findings (supplementary text 7). For example, the irrigation expansion dataset is based on historical data [22], while bioenergy potentials are quantified here for a 30 years average climate centered around the 2020s. We also considered a measurement based climate input to the yield model (supplementary figure 9). This led to highly comparable results in terms of sustainable potentials for rain-fed production and with small monthly water storages (−1.5% to +2.9% change, medium agricultural management). They differed somewhat more with the additional introduction of larger hard-path annual water storages (−6.7% change). It also led to increasing productive area extent (up to 4.4%), increases in green water use (up to 10%), and decreases in blue water use (down to −13%) for these scenarios. More research is needed to assess how bioenergy potentials are affected by changing crop productivity, water use, and irrigation opportunities under future climatic conditions.

The climate change mitigation benefits of bioenergy production on abandoned land will depend on the degree of natural regrowth since abandonment and bioenergy conversion technology [69]. Most of the abandoned land in the fSU has been under natural regrowth for nearly three decades with shrubs and young forests appearing in many locations [16, 70]. In general, the carbon accumulation has been slow in the fSU with few areas exceeding 5 Mg C ha<sup>-1</sup> and with the highest standing carbon stocks in the western parts of the region [70]. Bioenergy deployment should aim to target areas where bioenergy crop productivity and the climate benefits of fossil fuel substitution outperforms natural based solutions.

Deploying bioenergy crops on fSU abandoned land can contribute to close regional ambition gaps to meet the National Declared Contributions to the Paris Agreement [71], especially when bioenergy production is coupled with carbon capture and storage (BECCS) [14, 69, 72]. Perennial grasses can serve as an input to BECCS in thermal power plants or in biorefineries, as the biomass conversion processes involved produce exhaust CO<sub>2</sub> streams targetable for carbon capture [69, 72, 73]. Comparing our findings with future fSU land use projections in 2050 for 2 °C scenarios shows that rain-fed productive abandoned lands can meet 26%–61% of bioenergy land requirements across the SSPs (or 30%–80% with sustainable irrigation). A further deployment of bioenergy crops would require targeting present day cropland, pastures, or areas with primary vegetation. Future agricultural intensification or a reduction in land-based feed and food products through dietary changes would be needed to free lands for additional bioenergy production [2, 74].

While the hard-path irrigation strategy is sustainable in the sense that it accounts for environmental



flow protection [22], it also involves high capital costs and the construction of large water reservoir infrastructure that can be unsustainable by impacting habitats, displacing humans or altering hydrological regimes [75]. These factors must be accounted for in irrigation planning, and the smaller dams needed in the soft-path strategy have relatively lower risks of causing sustainability trade-offs. Any large-scale deployment of irrigation infrastructure would likely require policy support and incentives and should be accompanied by legislations aiming to ensure their sustainability.

Management of land and water resources stands at the heart of sustainable bioenergy deployment strategies. While irrigated bioenergy deployment increases bioenergy potentials with reduced land requirements, uncontrolled irrigation expansion risks causing water stress [7]. Our findings suggests that irrigation can be sustainably considered in up to 18 Mha of abandoned land. This can double bioenergy potentials relative to rain-fed conditions from 3.5 to 7.1 EJ yr<sup>-1</sup>, but involves using a large share of the remaining sustainably available blue water budget in the fSU (supplementary figure 10), thereby limiting the opportunity for new irrigated food production.

As recultivation is currently gaining momentum in the fSU [20, 76], the joint consideration of potential environmental and socio-economic co-benefits or trade-offs of land sparing and rain-fed or irrigated recultivation for food and bioenergy production is important to identify optimal land and water management practices at the local level. Assessments should determine how global challenges can be better addressed from the given local context. Using abandoned land to grow bioenergy crops is a favorable way of increasing bioenergy supply with reduced risks to food security and the environment. Nexus approaches integrating the multiple complex interactions between bioenergy potentials, and land and water use contributes to improved understanding of resource management and to shaping sustainable bioenergy deployment strategies.

### Data availability statements

The data that support the findings of this study are available upon reasonable request from the authors.

### Acknowledgments

We gratefully acknowledge the provision of GAEZ data by IIASA, GPWv4 data by NASA, lower heating values by Phyllis2, fSU land cover data [16, 32], sustainable irrigation expansion data [22, 56], GCAM-DEMETER land use projections [47], lignocellulosic bioenergy crop yields data [64, 66], and biodiversity hotspots data [45]. We thank Zhipin Ai for providing H08 yield data for switchgrass. H M was funded by


Research council of Norway project Bio4-7Seas (Project No. 302276) and the European Union's Horizon 2020 research and innovation programme under Grant Agreement No 869357, Project OceanNETs. Computations were performed on resources provided by Sigma2—the National Infrastructure for High Performance Computing and Data Storage in Norway (Account nn9518k).

### Conflict of interest

The authors declare no conflict of interest.

### ORCID iDs

Jan Sandstad Næss  <https://orcid.org/0000-0003-3166-913X>

Cristina Maria Iordan  <https://orcid.org/0000-0001-9975-2656>

Helene Muri  <https://orcid.org/0000-0003-4738-493X>

Francesco Cherubini  <https://orcid.org/0000-0002-7147-4292>

### References

- [1] Rogelj J *et al* 2018 Scenarios towards limiting global mean temperature increase below 1.5 °C *Nat. Clim. Change* **8** 325–32
- [2] IPCC 2019 Summary for policymakers *Climate Change and Land: An IPCC Special Report on Climate Change, Desertification, Land Degradation, Sustainable Land Management, Food Security, and Greenhouse Gas Fluxes in Terrestrial Ecosystems*
- [3] Vaughan N E and Gough C 2016 Expert assessment concludes negative emissions scenarios may not deliver *Environ. Res. Lett.* **11** 95003
- [4] Forster J, Vaughan N E, Gough C, Lorenzoni I and Chilvers J 2020 Mapping feasibilities of greenhouse gas removal: key issues, gaps and opening up assessments *Glob. Environ. Change* **63** 102073
- [5] Anderson K and Peters G 2016 The trouble with negative emissions *Science* **354** 182 LP—183
- [6] Jans Y, Berndes G, Heinke J, Lucht W and Gerten D 2018 Biomass production in plantations: land constraints increase dependency on irrigation water *GCB Bioenergy* **10** 628–44
- [7] Stenzel F, Greve P, Lucht W, Tramberend S, Wada Y and Gerten D 2021 Irrigation of biomass plantations may globally increase water stress more than climate change *Nat. Commun.* **12** 1512
- [8] Stenzel F, Gerten D, Werner C and Jägermeyr J 2019 Freshwater requirements of large-scale bioenergy plantations for limiting global warming to 1.5 °C *Environ. Res. Lett.* **14** 84001
- [9] D'Odorico P *et al* 2018 The global food-energy-water nexus *Rev. Geophys.* **56** 456–531
- [10] Ai Z, Hanasaki N, Heck V, Hasegawa T and Fujimori S 2021 Global bioenergy with carbon capture and storage potential is largely constrained by sustainable irrigation *Nat. Sustain.* **4** 884–91
- [11] Liu J *et al* 2018 Nexus approaches to global sustainable development *Nat. Sustain.* **1** 466–76
- [12] Næss J S, Cavalett O and Cherubini F 2021 The land–energy–water nexus of global bioenergy potentials from abandoned cropland *Nat. Sustain.* **4** 525–36

- [13] Johnson N *et al* 2019 Integrated solutions for the water-energy-land nexus: are global models rising to the challenge? *Water* **11** 2223
- [14] Muri H 2018 The role of large-scale BECCS in the pursuit of the 1.5 °C target: an Earth system model perspective *Environ. Res. Lett.* **13** 44010
- [15] Daioglou V, Doelman J C, Wicke B, Faaij A and van Vuuren D P 2019 Integrated assessment of biomass supply and demand in climate change mitigation scenarios *Glob. Environ. Change* **54** 88–101
- [16] Lesiv M *et al* 2018 Spatial distribution of arable and abandoned land across former Soviet Union countries *Sci. Data* **5** 180056
- [17] Lasanta T, Arnáez J, Pascual N, Ruiz-Flaño P, Errea M P and Lana-Renault N 2017 Space-time process and drivers of land abandonment in Europe *CATENA* **149** 810–23
- [18] Baumann M, Kuemmerle T, Elbakidze M, Ozdogan M, Radeloff V C, Keuler N S, Prishchepov A V, Kruhlov I and Hostert P 2011 Patterns and drivers of post-socialist farmland abandonment in Western Ukraine *Land Use Policy* **28** 552–62
- [19] Li S and Li X 2017 Global understanding of farmland abandonment: a review and prospects *J. Geogr. Sci.* **27** 1123–50
- [20] Prishchepov A V, Ponkina E V, Sun Z, Bavorova M and Yekimovskaja O A 2021 Revealing the intentions of farmers to recultivate abandoned farmland: a case study of the Buryat Republic in Russia *Land Use Policy* **107** 105513
- [21] Leirpoll M E, Næss J S, Cavalett O, Dorber M, Hu X and Cherubini F 2021 Optimal combination of bioenergy and solar photovoltaic for renewable energy production on abandoned cropland *Renew. Energy* **168** 45–56
- [22] Rosa L, Chiarelli D D, Sangiorgio M, Beltran-Peña A A, Rulli M C, D'Odorico P and Fung I 2020 Potential for sustainable irrigation expansion in a 3 °C warmer climate *Proc. Natl Acad. Sci.* **117** 29526 LP–29534
- [23] Stenzel F, Gerten D and Hanasaki N 2021 Global scenarios of irrigation water abstractions for bioenergy production: a systematic review *Hydrol. Earth Syst. Sci.* **25** 1711–26
- [24] Rockström J, Falkenmark M, Karlberg L, Hoff H, Rost S and Gerten D 2009 Future water availability for global food production: the potential of green water for increasing resilience to global change *Water Resour. Res.* **45** W00A12
- [25] Velpuri N M and Senay G B 2017 Partitioning evapotranspiration into green and blue water sources in the conterminous United States *Sci. Rep.* **7** 6191
- [26] Campbell J E, Lobell D B, Genova R C and Field C B 2008 The global potential of bioenergy on abandoned agricultural lands *Environ. Sci. Technol.* **42** 5791–4
- [27] Cai X, Zhang X and Wang D 2011 Land availability analysis for biofuel production *Environ. Sci. Technol.* **45** 334–9
- [28] Baxter R E and Calvert K E 2017 Estimating available abandoned cropland in the United States: possibilities for energy crop production *Ann. Am. Assoc. Geogr.* **107** 1162–78
- [29] Zumkehr A and Campbell J E 2013 Historical US cropland areas and the potential for bioenergy production on abandoned croplands *Environ. Sci. Technol.* **47** 3840–7
- [30] Lark T J, Meghan Salmon J and Gibbs H K 2015 Cropland expansion outpaces agricultural and biofuel policies in the United States *Environ. Res. Lett.* **10** 44003
- [31] Fischer G *et al* 2012 Global agro-ecological zones (GAEZ v3.0)-model documentation
- [32] Lesiv M *et al* 2017 Spatial distribution of abandoned arable land in former Soviet Union countries, link to map in GeoTIFF format. In supplement to: Lesiv M *et al* 2018 Spatial distribution of arable and abandoned land across former Soviet Union countries *Sci. Data* **5** 180056
- [33] Alcántara C *et al* 2013 Mapping the extent of abandoned farmland in Central and Eastern Europe using MODIS time series satellite data *Environ. Res. Lett.* **8** 35035
- [34] Estel S, Kuemmerle T, Alcántara C, Levers C, Prishchepov A and Hostert P 2015 Mapping farmland abandonment and recultivation across Europe using MODIS NDVI time series *Remote Sens. Environ.* **163** 312–25
- [35] Schierhorn F, Müller D, Beringer T, Prishchepov A V, Kuemmerle T and Balmann A 2013 Post-Soviet cropland abandonment and carbon sequestration in European Russia, Ukraine, and Belarus *Glob. Biogeochem. Cycles* **27** 1175–85
- [36] Prishchepov A V, Radeloff V C, Baumann M, Kuemmerle T and Müller D 2012 Effects of institutional changes on land use: agricultural land abandonment during the transition from state-command to market-driven economies in post-Soviet Eastern Europe *Environ. Res. Lett.* **7** 24021
- [37] Defourny P *et al* 2017 Land cover CCI product user guide version 2.0
- [38] Friedl M A, Sulla-Menashe D, Tan B, Schneider A, Ramankutty N, Sibley A and Huang X 2010 Remote sensing of environment MODIS collection 5 global land cover : algorithm refinements and characterization of new datasets *Remote Sens. Environ.* **114** 168–82
- [39] Kraemer R, Prishchepov A V, Müller D, Kuemmerle T, Radeloff V C, Dara A, Terekhov A and Frühauf M 2015 Long-term agricultural land-cover change and potential for cropland expansion in the former Virgin Lands area of Kazakhstan *Environ. Res. Lett.* **10** 54012
- [40] Jun C, Ban Y and Li S 2014 Open access to Earth land-cover map *Nature* **514** 434
- [41] Myers N, Mittermeier R A, Mittermeier C G, Fonseca G A B and Kent J 2000 Biodiversity hotspots for conservation priorities *Nature* **403** 853–8
- [42] WDPA 2009 *World database of protected areas* (Annual Release)
- [43] Folberth C, Khabarov N, Balković J, Skalský R, Visconti P, Ciaia P, Janssens I A, Peñuelas J and Obersteiner M 2020 The global cropland-sparing potential of high-yield farming *Nat. Sustain.* **3** 281–9
- [44] Hu X, Huang B, Veronesi F, Cavalett O and Cherubini F 2020 Overview of recent land-cover changes in biodiversity hotspots *Front. Ecol. Environ.* **19** 91–97
- [45] Hoffman M, Koenig K, Bunting G, Costanza J and Williams K J 2016 Biodiversity hotspots (version 2016.1) (<https://doi.org/10.5281/zenodo.3261807>)
- [46] Center for International Earth Science Information Network—CIESIN and Columbia University & Centro Internacional de Agricultura Tropical—CIAT Gridded population of the World, version 4 (GPWv4): national identifier grid (<https://doi.org/10.7927/H4TD9VDP>)
- [47] Chen M, Vernon C R, Graham N T, Hejazi M, Huang M, Cheng Y and Calvin K 2020 Global land use for 2015–2100 at 0.05° resolution under diverse socioeconomic and climate scenarios *Sci. Data* **7** 320
- [48] Calvin K *et al* 2019 GCAM v5.1: representing the linkages between energy, water, land, climate, and economic systems *Geosci. Model Dev.* **12** 677–98
- [49] Wise M, Calvin K, Kyle P, Luckow P and Edmonds J A E 2014 Economic and physical modeling of land use in GCAM 3.0 and an application to agricultural productivity, land, and terrestrial carbon *Clim. Change Econ.* **05** 1450003
- [50] Chen M, Vernon C R, Huang M, Calvin K V and Kraucunas I P 2019 Calibration and analysis of the uncertainty in downscaling global land use and land cover projections from GCAM using Demeter (v1.0.0) *Geosci. Model Dev.* **12** 1753–64
- [51] Vernon C R, Le Page Y, Chen M, Huang M, Calvin K V, Kraucunas I P and Braun C J 2018 Demeter—a land use and land cover change disaggregation model *J. Open Res. Softw.* **6**
- [52] Riahi K *et al* 2017 The shared socioeconomic pathways and their energy, land use, and greenhouse gas emissions implications: an overview *Glob. Environ. Change* **42** 153–68
- [53] van Vuuren D P *et al* 2011 The representative concentration pathways: an overview *Clim. Change* **109** 5

- [54] van Vuuren D P et al 2011 RCP2. 6: exploring the possibility to keep global mean temperature increase below 2 °C *Clim. Change* **109** 95–116
- [55] Chen M et al 2020 Global land use for 2015–2100 at 0.05° resolution under diverse socioeconomic and climate scenarios (Pacific Northwest National Laboratory) 2; PNNL (<https://doi.org/10.25584/data.2020-07.1357/1644253>)
- [56] Rosa L et al 2020 *Potential for sustainable irrigation expansion in a 3C warmer climate [Data set]* Zenodo (<https://doi.org/10.5281/zenodo.3995044>)
- [57] Jägermeyr J, Pastor A, Biemans H and Gerten D 2017 Reconciling irrigated food production with environmental flows for sustainable development goals implementation *Nat. Commun.* **8** 15900
- [58] Pastor A V, Ludwig F, Biemans H, Hoff H and Kabat P 2014 Accounting for environmental flow requirements in global water assessments *Hydrol. Earth Syst. Sci.* **18** 5041–59
- [59] Rosa L, Chiarelli D D, Rulli M C, Dell'Angelo J and D'Odorico P 2020 Global agricultural economic water scarcity *Sci. Adv.* **6** eaaz6031
- [60] Cox P M, Betts R A, Bunton C B, Essery R L H, Rowntree P R and Smith J 1999 The impact of new land surface physics on the GCM simulation of climate and climate sensitivity *Clim. Dyn.* **15** 183–203
- [61] New M, Lister D, Hulme M and Makin I 2002 A high-resolution data set of surface climate over global land areas *Clim. Res.* **21** 1–25
- [62] Mitchell T D and Jones P D 2005 An improved method of constructing a database of monthly climate observations and associated high-resolution grids *Int. J. Climatol.* **25** 693–712
- [63] ECN.TNO 2019 Phyllis2, database for (treated) biomass, algae, feedstocks for biogas production and biochar (available at: <https://phyllis.nl/>)
- [64] Li W et al 2020 Mapping the yields of lignocellulosic bioenergy crops from observations at the global scale *Earth Syst. Sci. Data* **12** 789–804
- [65] Ai Z, Hanasaki N, Heck V, Hasegawa T and Fujimori S 2020 Simulating second-generation herbaceous bioenergy crop yield using the global hydrological model H08 (v.bio1) *Geosci. Model Dev.* **13** 6077–92
- [66] Li W, Ciaia P, Makowski D and Peng S 2018 A global yield dataset for major lignocellulosic bioenergy crops based on field measurements *Sci. Data* **5** 180169
- [67] Olofsson P, Foody G M, Herold M, Stehman S V, Woodcock C E and Wulder M A 2014 Good practices for estimating area and assessing accuracy of land change *Remote Sens. Environ.* **148** 42–57
- [68] Liu J et al 2017 Water scarcity assessments in the past, present, and future *Earth's Future* **5** 545–59
- [69] Field J L et al 2020 Robust paths to net greenhouse gas mitigation and negative emissions via advanced biofuels *Proc. Natl Acad. Sci.* **117** 21968 LP–77
- [70] Meyfroidt P, Schierhorn F, Prishchepov A V, Müller D and Kuemmerle T 2016 Drivers, constraints and trade-offs associated with recultivating abandoned cropland in Russia, Ukraine and Kazakhstan *Glob. Environ. Change* **37** 1–15
- [71] Roelfsema M et al 2020 Taking stock of national climate policies to evaluate implementation of the Paris Agreement *Nat. Commun.* **11** 2096
- [72] Hanssen S V, Daioglou V, Steinmann Z J N, Doelman J C, van Vuuren D P and Huijbregts M A J 2020 The climate change mitigation potential of bioenergy with carbon capture and storage *Nat. Clim. Change* **10** 1023–9
- [73] Liu G, Larson E D, Williams R H, Kreutz T G and Guo X 2011 Making Fischer–Tropsch fuels and electricity from coal and biomass: performance and cost analysis *Energy Fuels* **25** 415–37
- [74] van Vuuren D P, Bijl D L, Bogaart P, Stehfest E, Biemans H, Dekker S C, Doelman J C, Gernaat D E H J and Harmsen M 2019 Integrated scenarios to support analysis of the food–energy–water nexus *Nat. Sustain.* **2** 1132–41
- [75] Gleick P H 2003 Global freshwater resources: soft-path solutions for the 21st century *Science* **302** 1524–8
- [76] Kamp J 2014 Weighing up reuse of Soviet croplands *Nature* **505** 483